Spectral characterization of the fluorescent components present in humic substances, fulvic acid and humic acid mixed with pure benzo(a)pyrene solution

Rawa El Fallah, Régis Rouillon, Florence Vouve

Spectral characterization of the fluorescent components present in humic substances, fulvic acid and humic acid mixed with pure benzo(a) pyrene solution

Rawa El Fallah, Régis Rouillon, Florence Vouvé *

Univ. Perpignan Via Domitia, Biocapteurs-Analyses-Environnement, 66860 Perpignan, France
Laboratoire de Biodiversité et Biotechnologies Microbiennes, USR 3579 Sorbonne Universités (UPMC) Paris 6 et CNRS Observatoire Océanologique, 66650 Banyuls-sur-Mer, France

ABSTRACT

The fate of benzo(a)pyrene (BaP), a ubiquitous contaminant reported to be persistent in the environment, is largely controlled by its interactions with the soil organic matter. In the present study, the spectral characteristics of fluorophores present in the physical fractions of the soil organic matter were investigated in the presence of pure BaP solution. After extraction of humic substances (HSs), and their fractionation into fluvic acid (FA) and humic acid (HA), two fluorescent compounds (C_1 and C_2) were identified and characterized in each physical soil fraction, by means of fluorescence excitation-emission matrices (FEEMs) and Parallel Factor Analysis (PARAFAC). Then, to each type of fraction having similar DOC content, was added an increasing volume of pure BaP solution in attempt to assess the behavior of BaP with the fluorophores present in each one. The application of FEEMs-PARAFAC method validated a three-component model that consisted of the two resulted fluorophores from HSs, FA and HA (C_1 and C_2) and a BaP-like fluorophore (C_3). Spectral modifications were noted for components C_2HSs (C_2 in humic substances fraction) (λex/λem: 420/490–520 nm), C_2FA (C_2 in fulvic acid fraction) (λex/λem: 400/487(517) nm) and C_1HA (C_1 in humic acid fraction) (λex/λem: 350/452(520) nm). We explored the impact of increasing the volume of the added pure BaP solution on the scores of the fluorophores present in the soil fractions. It was found that the scores of C_2HSs, C_2FA, and C_1HA increased when the volume of the added pure BaP solution increased. Superposition of the excitation spectra of these fluorophores with the emission spectrum of BaP showed significant overlaps that might explain the observed interactions between BaP and the fluorescent compounds present in SOM physical fractions.

1. Introduction

Polycyclic aromatic hydrocarbons (PAHs), which are compounds formed by the fusion of benzene rings consisting only of carbon and hydrogen, are important environmental pollutants of big concern because many of them are carcinogens and mutagens [1,2]. They originate from a variety of natural and anthropogenic sources. Particular attention has been made on the PAHs with high-molecular mass, such as benzo(a) pyrene (BaP), for their toxicological aspect [3,4]. BaP was reported as an indicator of the presence of other PAHs in different environmental compartments (water, soil, sediments) [5]. It is persistent in the environment, part because of its low bioavailability and because of its strong adsorption onto the soil organic matter (SOM) [6]. This strong interaction with SOM makes it un-degradable and unavailable resulting in soil contamination problems.

Soil organic matter, a key factor in the sustainability of soil, is composed mainly of humic substances (HSs) and nonhumic substances [7,8]. HSs are a complex mixture of several heterogenous aggregates [9]. HSs can be fractioned into humin, a black colored fraction insoluble in water at any pH; the humic acid (HA), black or brown, soluble in basic medium and insoluble in acidic pH (<2), and the fulvic acid (FA), yellowish and soluble in water at any pH [10]. HA is composed of natural polydispersed polyelectrolyte bio-colloids [11,12] and are characterized by the presence of many functional groups such as carboxylic acids, phenols and amines [9]. FA is characterized by small molecular size and large carboxyl group [13]. HA and FA contain also quinone and semi-quinone function groups [14,15]. Studies have shown that soil organic matter is predominant in the sorption of PAHs; it largely controls the fate of these pollutants [16]. PAHs were found to associate with the hydrophobic regions of soil organic matter because they have low solubility in water [17]. Binding affinity, expressed as the partition coefficient (Koc), was found correlated with aromaticity of the organic matter [18]. Thus, the hydrophobicity of the pollutant and the quality of the soil organic matter determine the nature of the interactions

occurring between them and define the extent of pollutant's bioavailability and toxicity [19,20]. Since SOM has a complex structure that is difficult to characterize, studies have used the physico-chemical properties such as the spectral properties to characterize and define HSs, HA and FA [21], and particularly the fluorescence spectroscopy method [22].

The fluorescence spectroscopy, especially the development of fluorescent excitation-emission matrixes (FEEMs) [23,24], have been widely used over the last decade to obtain information on the fluorescent characteristics of organic matter, to determine its origin and to assess its quality in different ecosystems [25–28]. The popularity of this method is due to the fact that it is a highly sensitive and nondestructive method that does not require a large amount of preparation time, the fast data acquisition and the large amount of information on the molecular structure and chemical properties of natural organic matter it provides [29–33]. However, in order to interpret and decompose the FEEMs, chemometric algorithms such as Parallel Factor Analysis (CP/PARAFAC) are frequently used [34–38]. PARAFAC is an advanced multivariate statistical technique that has been employed in the area of analytical and environmental chemistry; it is often utilized for the analysis of the three-way data sets [39] such as sample with x excitation wavelength y emission wavelength resulted from FEEMs [40–42]. It can identify and quantify the components of a multicomponent system and is able to extract their relative concentration and their pure excitation and emission spectra [43,44]. The combination of FEEMs with the PARAFAC algorithm is widely used to characterize the organic matter from terrestrial origin [22,37,45], aquatic origin [32,42,46]. Several authors have also proven the efficiency of this method to detect PAHs in pure solutions [36], in water samples [34], aqueous motor oil extract and asphalt leachate [34,36,47]. This technique makes it possible to observe the qualitative changes in the dissolved organic matter and the different fluorophores present in the tested samples and to detect changes in their fluorescence intensities [42].

FEEMs-PARAFAC method used for detection and quantification of PAHs in environmental matrices [35,48] can also be applied for understanding the interactions between SOM and organic pollutants, such as BaP, which is crucial for assessing their fate in soil environment. Since it is a novel method, there is currently no information available in literature about the effect of BaP on the spectral characteristics of the fluorophores present in each soil fraction HSs, FA and HA. In this study we combined FEEMs and PARAFAC to (1) determine the spectral characteristics of the fluorophores present in the three physical fractions HSs, FA and HA originating from one soil (2) investigate the effect of the addition of pure BaP solution on the spectral properties of the fluorophores present in HSs, FA, and HA, (3) explore the changes in fluorescence intensities of each fluorophore when the volume of added pure BaP solution increases and (4) clarify the physico-chemical interactions between BaP and the fluorophores present in each soil fraction.

2. Materials and Methods

2.1. Preparation of Pure BaP Solution

BaP was purchased from Sigma-Aldrich (≥96%) and was used without further purification. A stock solution of pure BaP (10^{-4} M) was produced by weighing the appropriate amount of BaP and dissolving it in ethanol (Carlo Erba HPLC grade). The stock solution was kept in the dark at 4 °C. A 10^{-5} M BaP solution was prepared in ultra-pure water by diluting the stock solution. This solution was used for the experiments with SOM. Triplet concentrations of 10^{-9}; $2 \cdot 10^{-9}$ and $5 \cdot 10^{-9}$ M of pure BaP solutions were also prepared in ultra-pure water to be used as calibration range to be inserted in the PARAFAC models. Ultra-pure water was taken from an Osmodem water purification unit.

2.2. SOM Extraction and Fractionation

An acidic brown soil sample was collected between 5 and 20 cm in depth from a non-polluted remote area of a high mountain (altitude of 1.657 m) located in the Pyrénées-Orientales department in southern France (42.52649°N; 2.12305°E). SOM was extracted from soil sample in alkaline conditions using an adaptation of Duchaufour and Jacquin [49] protocol, that was later completed by Ratsimbazafy [50]. Briefly, 10 g aliquots of dried (24 h at 105 °C) crushed and homogenized soil sieved through 2 mm mesh, were mixed in PETE bottle with a solution containing 80 mL of 0.1 M NaOH (Sigma-Aldrich) and 120 mL of 0.1 M $Na_4P_2O_7$ (Sigma-Aldrich) to reach a pH around 13. To obtain a correct homogenization, the bottle was put on a rotating agitator in the dark for 24 h. The mixture was then centrifuged at 3600g for 20 min. The supernatant thus obtained is the humic substances (HSs) fraction. One part of HSs was stored at room temperature in the dark for analysis. The other part was used to separate the FA and the HA fractions. Concentrated HCl (37%, Fulka) was added to HSs, up to pH < 2 and the solution was kept in the dark. After 24 h, a precipitate was observed. This solution was centrifuged at 3600g for 20 min to obtain FA fraction (supernatant) and the HA fraction (precipitate). Prior to analysis, HA was solubilized by adding 50 mL of pure water and agitating till solubilization. The pH of HSs, FA and HA solutions were adjusted to 7.5 ± 0.1. Prior to fluorescence measurements, samples were filtered through a 0.45 μm filters (PTFE-membrane from Sartorius Stedim Biotech).

2.3. Sample Preparation

Reference samples were obtained by preparing five solutions of HSs, FA and HA with different concentrations estimated on their dissolved organic carbon (DOC) contents. Concentrations of DOC were determined using Shimadzu Total Organic Carbon Analyzer V_{CSN} (Shimadzu Corp., Kyoto, Japan). Concentrations of HSs samples were 2.71, 4.71, 7.72, 15.75, 18.22 and 22.11 mg DOC·L^{-1} those of FA were 2.693, 3.209, 3.908, 7.779 and 17.48 mg DOC·L^{-1} and those of HA samples were 6.788, 9.212, 13.5, 17.2 and 20.14 mg DOC·L^{-1}.

As for the experiments with pure BaP, we selected the concentration of each soil fraction having DOC ± 7 mg·L^{-1}. For each fraction, triplicates with 3 mL of solution (~7 mg DOC·L^{-1}) were prepared. 100, 200 and 300 μL of pure BaP solution (10^{-5} M) was added to the first, the second and the third replicates respectively. The triplicates containing the mixture HSs-BaP, FA-BaP and HA-BaP thus obtained constitute three sets of samples that will be named as HSs$_{BaP}$, FA$_{BaP}$ and HA$_{BaP}$.

2.4. Fluorescence Spectroscopy

Fluorescence measurements were acquired using a SAFAS flx spectrofluorometer (SAFAS, Monaco) with a Xenon excitation source (150 W) using 1 cm × 1 cm quartz cell. All further measurements were performed at room temperature (20 °C $\pm$ 2 °C). FEEMs were recorded at 270 nm·min^{-1} scan speed. The excitation wavelengths ranged from 200 to 500 nm at 10 nm steps. Emission wavelengths ranged from 220 to 800 nm at 1 nm interval. Excitation and emission slit widths were set at 10 nm. Raman and Rayleigh diffusions were corrected by subtraction of ultra-pure water FEEM from each FEEMs' sample [31]. We have checked that there were no inner filter effects over each sample. Fluorescence intensities are expressed in arbitrary units (a.u.).

2.5. Data Analysis

PARAFAC has been widely described in the literature [41,42,44,52,55] hence, we will briefly describe it. It is applied to a three-way data X that have the trilinear structure such as in the case of FEEM. X, in this case, is a 3-way data cube of dimension I × J × K

and its trilinear decomposition using PARAFAC analysis can be expressed using the following equation

$$X_{i,j,k} = \sum_{f=1}^{F} a_{i,f} b_{j,f} c_{k,f} + \varepsilon_{i,j,k} \qquad (1)$$

The principle of PARAFAC decomposition is minimizing the sum of square of the residual; (ε_{ijk}) based on a least-squares algorithm which represents some additional residual variation not accounted for by the model. x_{ijk} is the intensity of fluorescence for the ith sample at emission wavelength j and excitation wavelength k. a_{if} is the relative concentration of analyte f in sample i; b_{jf} is linearly related to the fluorescence intensity of the fth fluorophore at emission wavelength j, c_{kf} is linearly related to the extinction coefficient of analyte f at excitation wavelength k and ε_{ijk} represents the sum of the residuals of the matrices. The PARAFAC model was calculated using a homemade program (progmeef), developed and provided by R. Redon (PROTEE Laboratory, University of Toulon, France) based on Matlab (TM) software. In order to reduce the effect of diffusion and scatter lines, the Rayleigh and Raman scatter were removed according to Zepp [58]. FEEMs were normalized and the data set was fitted with non-negativity constraint and was run for 100 iterations with initialization by random values for all data sets with a convergence criterion of 10^{-6}. A series of PARAFAC model from two to five components were fitted to the data.

The FEEMs of the reference samples of HSs, FA, and HA were modeled in three separate PARAFAC analyses. The FEEMs of the three sets of triplicates containing the mixture with pure BaP solution (HSs_{BaP}, FA_{BaP} and HA_{BaP}) were also run by PARAFAC.

The results were validated using core consistency diagnostic (CorConDia) [40]. The similarity coefficient, also known as congruence coefficient (r_c) of the computed and the reference two-dimensional fluorescence spectra was calculated according to [59]:

$$r_c = \frac{\sum ab}{\sqrt{\left(\sum a^2 \sum b^2 \right)}} \qquad (2)$$

where a and b represent the loadings of computed and reference spectrum respectively. In our study, the computed spectra were obtained from the PARAFAC calculations of the three sets of HSs_{BaP}, FA_{BaP}, HA_{BaP} and, the reference spectra are obtained from the PARAFAC model of the three reference sets of HSs, FA and HA. This congruence coefficient allows the estimation of the modification of the spectral characteristics of the reference fluorophores from reference sets when pure BaP is added to the soil fractions. An $r_c = 0.90$ indicates a high level of similarity, values higher than 0.95 indicate that the compared spectra are virtually identical.

3. Results and Discussion

3.1. Characterization of the Fluorescent Reference Components in HSs, FA and HA

The appropriate number of components resulting from PARAFAC model was determined by high values of CorConDia and by visual analysis of the spectra of the obtained components. The PARAFAC models tested with 3, 4 and 5 components were excluded because of the low values of CorConDia combined with inappropriate spectral shapes. The best PARAFAC test was obtained from the two-component model. Results showed the contribution of two fluorophores in each soil fraction with a CorConDia of 96%, 94% and 99% for HSs, FA and HA respectively. Fig. 1 shows the spectra of two fluorophores present in the reference HSs, FA and HA. The spectral characteristics of the components C_1 and C_2 present in HSs, FA and HA showed similarities with previous fluorophores reported in literature (Table 1). Component C_1HSs and C_1FA from this study had similar spectral characteristics with component 1 found in estuarine system by Singh et al. [51], and in aquatic environments by Stedmon et al [52] and by Nagao et al [54] and other works listed in Table 1. Component C_2HSs and C_2FA were found similar to component 4 in estuary from Singh et al. [51] study and component 2 from Stedmon et al. and Stedmon and Markager works found in estuary and sea water respectively [42,55]. C_1HA (λex/λem: 350/452 nm) refers to humic-like component (C-peak) [24] in marine environment and to HA in coral reefs [56]. Component C_2HA (λex/λem: 460/(496) 520 nm) refers to soil fulvic acid [52] in aquatic environment, to component 2 in whole soil and humin samples [38] to terrestrial HA and lignin derivatives [56] and to Aldrich HA [57].

We used similarity coefficient (r_c) and visual observations (Fig. 2) to compare the similarity of the spectral characteristics between C_1HSs and C_1FA and between C_2HSs and C_2FA. C_1HSs and C_1FA have similar PARAFAC excitation and emission loading spectra and recorded a congruence coefficient $r_c = 0.996$ for both excitation and emission (Fig. 2A). The excitation spectra of C_2HSs and C_2FA recorded a similarity coefficient of 0.968; the peak of C_2HSs maximum around 420 nm was broader than that of C_2FA maximum at 400 nm (Fig. 2B). The emission spectra of these two components recorded a high similarity coefficient of 0.974 with a common peak at 490 and 487 nm respectively and a second peak at 520 nm for C_2HSs which becomes a shoulder at 517 nm for C_2FA. Excitation and emission spectra of C_1HA had similar shapes comparing to those of C_1HSs and C_1FA with a red shift around 20 nm (Fig. 2A) (λex/λem: 350/452(520) nm). Its emission shoulder at 520 nm is much more apparent than in C_1HSs and C_1FA (517 nm).

As seen in Fig. 2B, C_2HA had less similar excitation spectral loading to those of C_2HSs ($r_c = 0.956$) and C_2FA ($r_c = 0.927$). The similarity coefficients of the emission spectral loading of C_2HA with the emission spectral loadings of C_2HSs and C_2FA were 0.966 and 0.942 respectively. The shoulder of C_2HA (496 nm) corresponded to common peaks in C_2HSs
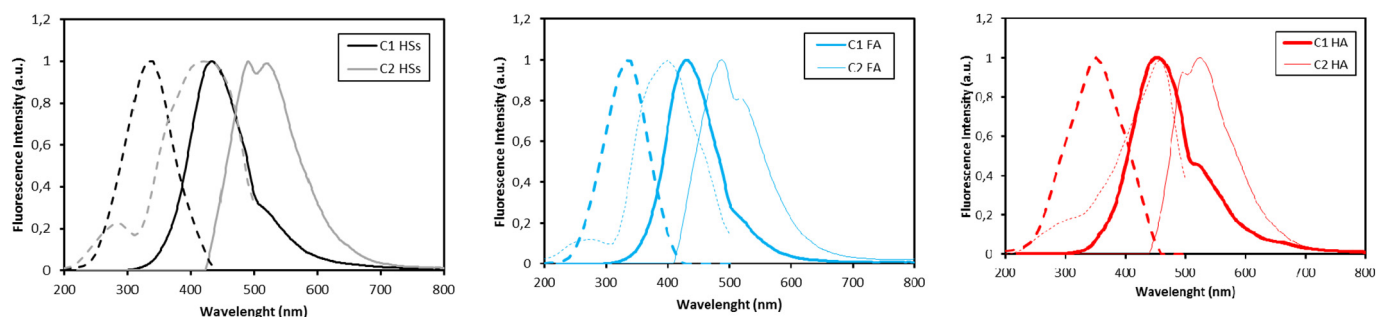

Fig. 1. Normalized excitation (dashed line) and emission (solid line) spectral loadings obtained from independent two components (C1 and C2) PARAFAC model from reference fractions HSs, FA and HA.

Component (this study)	Ex/Em (nm)	References
Component C_1HSs	330/433(520)	Component 1 [51]
C_1FA	330/430(520)	Component 1 [52]
		Component 1 [53]
		Component 4 [42]
		Component 1 [32]
		Component 3 [22]
		FA [54]
Component C_2HSs	420/490–520	Component 4 [51]
C_2FA	400/487(517)	Component 2 [42]
		Component 2 [55]
Component C_1HA	350/452(520)	C-peak Humic-like [24]
		Component 3 [52]
		Component 1 [42]
		Component 1 [22]
		HA [56]
Component C_2HA	460/(496)520	Component 4 [54]
		Component 2 [38]
		E soil fulvic acid [52]
		Terrestrial HA [56]
		HA Aldrich [57]

(490 nm) and C_2FA (497 nm). The peak around 520 nm is common for C_2HSs and C_2HA while a shoulder was observed for C_2FA at similar wavelength (517 nm). On the other hand, excitation and emission spectra of C_2HSs seem to be a combination of those of C_2FA and C_2HA.

3.2. PARAFAC Decomposition of HSs, FA and HA Containing Pure BaP

The best PARAFAC analysis applied to FEEMs of tested soil fractions with added BaP (HSs_{BaP}, FA_{BaP} and HA_{BaP}) revealed the presence of three components (Fig. 3B). CorConDia scored 94%, 91% and 41% for PARAFAC decomposition of HSs_{BaP}, FA_{BaP} and HA_{BaP} respectively. Despite a weak CorConDia, the three factor PARAFAC model of HA_{BaP} was validated because the spectral characteristics of the three components were consistent with those validated in HSs_{BaP} and FA_{BaP}. The decompositions to more than three components did not score a high CorConDia percentage (<40%).

The spectral characteristics of the three fluorophores found in HSs_{BaP} and FA_{BaP} are very similar with similarity coefficients above 0.950. C_1HSs_{BaP} and C_1FA_{BaP} had their excitation and emission maxima ($\lambda ex/\lambda em$) at 340/430 nm ($r_c = 0.996$ for the excitation spectra and $r_c = 0.998$ for the emission spectra) and C_2HSs_{BaP} and C_2FA_{BaP} had their

maxima and (shoulder) at 400/(494) 525 nm and 400/(495) 526 nm respectively ($r_c = 0.997$ for the excitation spectra and $r_c = 1$ for the emission spectra). C_3HSs_{BaP} and C_3FA_{BaP} had their $\lambda ex/\lambda em$ maxima at 290–380/408–427 nm ($r_c = 0.999$ for the excitation spectra and the emission spectra).

The spectral shape of component C_1HA_{BaP} spectra ($\lambda ex/\lambda em$: (360) 400/492–526 nm) differ from those of HSs_{BaP} and FA_{BaP} with a red shift of around 60 nm. C_2HA_{BaP} excitation spectrum (maxima at λex: 470 nm) differ from those of C_2HSs_{BaP} and C_2FA_{BaP} in shape and location and recorded a red shift of around 70 nm. Whereas the emission spectrum of C_2HA_{BaP} (λem at (495)525 nm), was found similar to those found in HSs_{BaP} and FA_{BaP} having the same peak location but has a narrower shape, their similarity coefficient were 0.928 for C_2HSs_{BaP} and 0.926 for C_2FA_{BaP}. The shape of the excitation and emission spectra of C_3HA_{BaP} are slightly modified comparing to those of C_3HSs_{BaP} and C_3FA_{BaP} and had maxima at $\lambda ex/\lambda em$ at 300–370/409–427 nm. The congruence coefficient r_c of the excitation spectra of C_3HA_{BaP} with C_3HSs_{BaP} and C_3FA_{BaP} are scored 0.958 and 0.950 respectively and those of the emission spectra of C_3HA_{BaP} with C_3HSs_{BaP} and C_3FA_{BaP} scored 0.976 and 0.981.

On the other hand, by comparison with the spectral properties of pure BaP (10^{-5} M) in water, the third fluorophore (C_3HSs_{BaP}; C_3FA_{BaP}; C_3HA_{BaP}) was identified as BaP. The similarity coefficient r_c of the excitation spectral loading of components C_3HSs_{BaP} and C_3FA_{BaP} with that of pure BaP were 0.995 and 0.991 respectively and those of the emission spectral loadings were of 0.984 and 0.985 respectively. C_3HA_{BaP} was also identified as BaP having a similarity coefficient r_c of 0.972 and 0.988 for the excitation and emission spectral loadings respectively.

Regardless of the high similarity coefficient between the spectral characteristics of C_3HA_{BaP} and pure BaP, it can be visually noticed that there are some deformations in the shape of C_3 spectral loadings in HA_{BaP}. That seems to reveal a modification of the spectral characteristics of BaP in HA_{BaP} fraction.

Thus the presence of BaP affects the spectral characteristics of soil fractions conserving fluorescent feature of pure BaP in HS and FA fractions but not in HA fraction where fluorescence of BaP is modified compared to that of pure form.

Comparison of PARAFAC spectral loadings of reference components (Fig. 3A) resulting from the separate decomposition of HSs, FA and HA with those resulting from decomposition of HSs_{BaP}, FA_{BaP} and HA_{BaP} containing added pure BaP (Fig. 3B) shows that BaP modified the fluorescence features of each fraction differently.

For C_1, spectral modifications due to the addition of pure BaP are identical in HSs and FA fractions which have highly similar spectral characteristics as previously mentioned. It was noted that the resulting
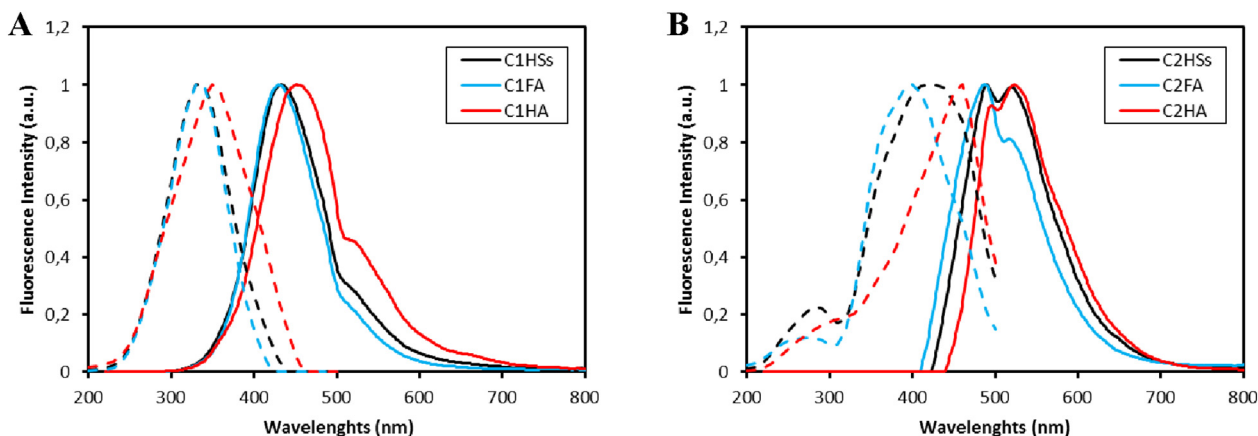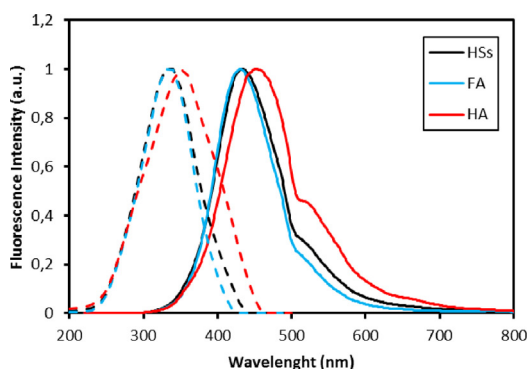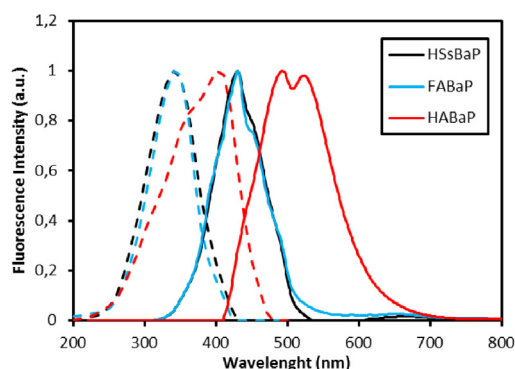

Fig. 2. Comparison of spectral characteristics of the obtained fluorophores (C1 and C2) from two component PARAFAC model in HSs, FA and HA (normalized spectra).
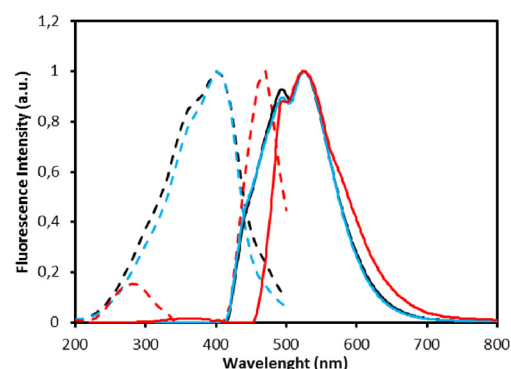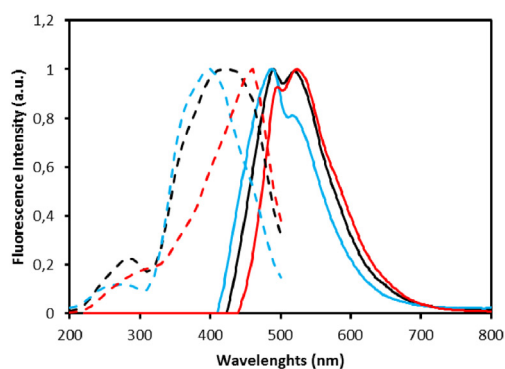
A-Reference components of HSs, FA and HA

B-Components of HSs_{BaP}, FA_{BaP} and HA_{BaP}
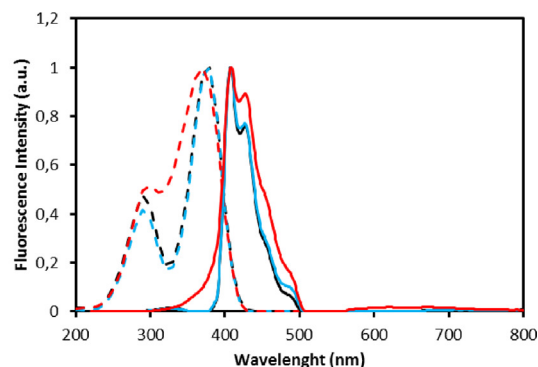
C1

C2

C3

Fig. 3. A. Normalized excitation (dashed) and emission (solid lines) spectral loadings of two component PARAFAC model of reference HSs, FA and HA. B. Normalized excitation (dashed) and emission (solid lines) spectral loadings of three-component PARAFAC model of HSs$_{BaP}$, FA$_{BaP}$ and HA$_{BaP}$ (C1: component 1, C2: component 2 and C3: component 3).

excitation spectra of C$_1$HSs$_{BaP}$ and C$_1$FA$_{BaP}$ were red shifted by 10 nm in comparison with those from the reference data sets C$_1$HS and C$_1$FA. Despite the red shift and the modified shape, the excitation and emission spectral loading of components C$_1$HSs$_{BaP}$ scored a congruence coefficient r$_c$ = 0.995 and r$_c$ = 0.968 with those of the reference C$_1$HS. Comparing the spectral loadings of C$_1$FA$_{BaP}$ with those of the reference C$_1$FA, similarity coefficient r$_c$ recorded 0.990 for excitation and emission.

Comparing the spectral features of C$_1$HA and C$_1$HA$_{BaP}$, we noted a modification in the shape of the excitation and emission spectra of

C$_1$HA$_{BaP}$ along with a red shift of 50 nm for the λex and 40 nm for λem. The congruence coefficient r$_c$ of the compared excitation spectra was r$_c$ = 0.910 and that of the emission spectra recorded a lower value (r$_c$ = 0.789) that was due to the appearance of the double peak (λem: 492–523 nm) (Fig. 3B).

Spectral characteristics of the excitation and emission loadings of components C$_2$HSs$_{BaP}$ and C$_2$FA$_{BaP}$ were also compared to those of C$_2$HSs and of C$_2$FA. It was found that the emission spectral loadings of C$_2$HSs$_{BaP}$ and C$_2$FA$_{BaP}$ were similar to those of the reference and scored similarity coefficients r$_c$ = 0.994 and 0.980 respectively. The intensity of

the peak around 490 nm decreased, while the intensity of the peak around 520 nm increased in C_2HSs_{BaP} and C_2FA_{BaP}. The excitation spectral loadings of C_2HSs_{BaP} and C_2HSs were less similar and had a similarity coefficient $r_c = 0.903$, whereas those of C_2FA_{BaP} and C_2FA showed higher similarity and scored an $r_c = 0.956$. It was also noticed that the λex of C_2HSs_{BaP} had a blue shift of around 20 nm compared with λex of C_2HSs along with a modified shape.

In HA_{BaP} fraction, the shape of the excitation spectra of C_2HA_{BaP} was modified and red shifted by 10 nm compared with that of C_2HA. Similarity coefficient of the excitation spectra of C_2HA_{BaP} and C_2HA was weak ($r_c = 0.814$). However, the addition of BaP had little effect on the emission spectrum of C_2HA_{BaP}. It recorded a high similarity coefficient (0.980) with that of C_2HA.

These comparisons demonstrated that the presence of BaP seems to highly influence the fluorescence features of C_1 in HA fraction while the fluorescence characteristics of C_2 seem to be more affected by BaP in HSs and FA fractions.

3.3. BaP Impact on the Fluorophores in Soil Fractions

The influence of BaP on the fluorophores present in soil was studied through the addition of 100, 200 and 300 μL of pure BaP (10^{-5} M) to 3 mL of HSs, FA and HA. Fig. 4 shows the relative scores of components from PARAFAC in the three tested fractions. The addition of BaP to HSs and FA led to a high increase in fluorescence intensity of C_2HSs_{BaP} (slope = 1713.4) and C_2FA_{BaP} (slope = 1597.1). They had steeper slopes compared to those of C_1HSs_{BaP} (340.07) and C_1FA_{BaP} (133.82). The scores of C_2HA_{BaP} did not increase with the addition of BaP (slope = 74.372). On the other hand, C_1HA_{BaP} recorded a high slope (1188.2). These results confirm the influence of BaP addition on fluorescence intensities increase of C_2 in HSs_{BaP} and FA_{BaP} fractions and of C_1 in HA_{BaP} fraction. The behavior of C_3, identified as BaP, is logically related to the addition of pure BaP with a high increase of relative scores (slope = 1216.2) in HSs_{BaP} fraction. The behavior of C_3HSs_{BaP} is similar to the variation of C_2HSs_{BaP} (slope = 1713.4). In FA_{BaP} data sets, the increase of C_3 relative scores is lower (slope = 617.5) than that in HSs_{BaP}. This behavior of C_3FA_{BaP} shows a moderate variation compared to the high evolution of C_2FA_{BaP} (slope = 1597.1). The lowest increase of C_3 relative scores is observed in HA_{BaP} fraction (slope = 332.27) which differs from the high variation of C_1HA_{BaP} (slope = 1188.2).

This attenuation of C_3 fluorescence intensities in FA_{BaP} and mainly in HA_{BaP} fractions could be due to interactions between BaP and these fractions. As reported in previous studies, HA was found to be a fluorescent quencher that can reduce the fluorescence intensity of PAHs such as phenanthrene, pyrene, anthracene [48], naphthalene [60] and fluoranthene [61]. So quenching effect could have caused the attenuation of
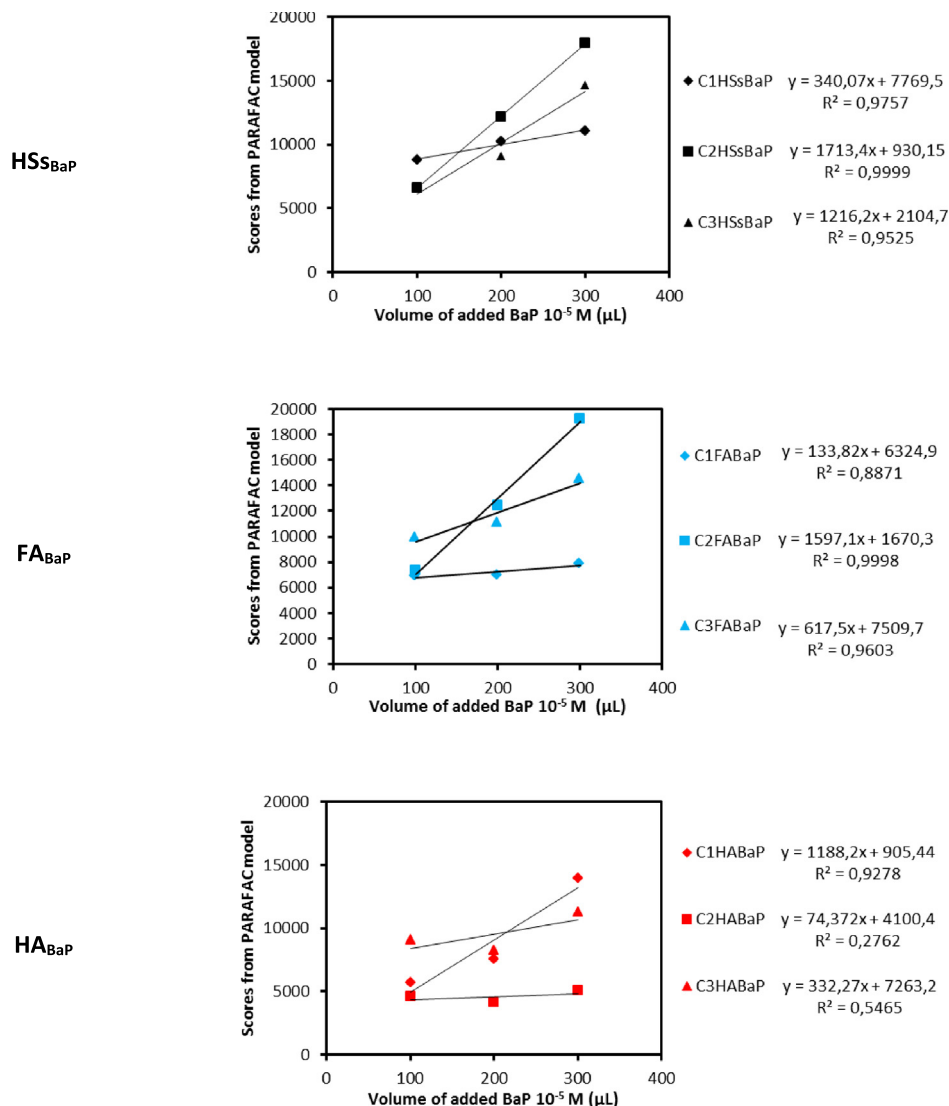

Fig. 4. Correlation of PARAFAC loading scores of components present in HSs_{BaP}, FA_{BaP} and HA_{BaP} with increasing volume of pure BaP (10^{-5} M) in water.

the fluorescence intensities of C_3HA_{BaP} in HA fraction in our study. Perhaps this phenomenon could have also occurred in a less intensive way in FA_{BaP} fraction.

By taking into consideration the higher variations of fluorescence intensity of C_2HSs, C_2FA, and C_1HA compared to those of C_3HSs, C_3FA, and C_3HA, it is possible to interpret these results as fluorescence resonance energy transfer (FRET). Superposition of the excitation and the emission spectra of pure BaP and those of the reference components present in HSs, FA and HA were carried out because the existence of overlaps between emission spectra of one component (energy donor) with the excitation spectra of another (energy acceptor) might induce energy transfer that in turn influences the fluorescence intensities. The fluorescence intensity of the energy donor shall decrease while that of the acceptor will increase. The superposition showed that the excitation

spectra of components C_2HSs and C_2FA completely covers the emission spectra of pure BaP (Fig. 5A and B). The energy from the emission of BaP (donor) might have been transferred to the excitation of C_2HSs and C_2FA (acceptors). It is also noted that the emission spectra of pure BaP overlaps the end of the excitation spectra of C_1HA, and the beginning of the excitation spectra of C_2HA (Fig. 5C). As only C_1HA_{BaP} fluorescence intensities increased (Fig. 4), this might propose that C_1HA gained energy from the emission of pure BaP.

4. Conclusion

We studied by means of FEEMs-PARAFAC method, the spectral characteristics of the fluorescent components present in the SOM physical fractions HSs, FA and HA originating from a single soil sample. Then we investigated their spectral properties upon the addition of pure BaP solution to obtain new information regarding the interactions of BaP with these fluorophores.

HSs and FA fractions had one component (C1) highly similar. Upon addition of pure BaP solution component C_2HSs and C_2FA recorded similar spectral modifications.

Increasing the added volume of pure BaP solution allowed us to evaluate the variations of the scores resulting from PARAFAC model. These scores variations were also similar for HSs and FA fraction. We noticed that the scores of C_2HSs and C_2FA increased when the volume of added pure BaP solution increased.

The fluorophores present in HA fraction did not show high similarity with those present in HSs and FA except for the emission of C_2HA that was quite close to those of C_2HSs and C_2FA. The addition of pure BaP solution resulted in spectral modification of component C_1HA and when the volume of BaP increased, the scores of this fluorophore increased as well.

The superposition of the excitation spectral loadings of C1 and C2 with the emission spectra of BaP in this study showed that BaP might be an energy donor and C_2HSs, C_2FA, and C_1HA might be energy acceptors. Further complementary analysis using time-resolved fluorescence technique could support these observations.

This work showed that MEEFs-PARAFAC method can be applied for monitoring the quality of soils and for evaluating of the fate of polycyclic aromatic hydrocarbon such as benzo(a)pyrene in the humic substances, fulvic acid and humic acid.

Fig. 5. Superposition of the normalized excitation spectra obtained from a two-component PARAFAC model of reference HSs, FA and HA fractions and the normalized emission spectra of pure BaP.

References

[1] M. Lee, Analytical Chemistry of Polycyclic Aromatic Compounds, Elsevier Science, Burlington, 2012.
[2] R.G. Harvey, Polycyclic Aromatic Hydrocarbons, Wiley [u.a.], New York, 1997.
[3] B. Armstrong, C. Tremblay, D. Baris, G. Thériault, Lung cancer mortality and polynuclear aromatic hydrocarbons: a case-cohort study of aluminum production workers in Arvida, Quebec, Canada, Am. J. Epidemiol. 139 (1994) 250–262.
[4] W.B. Wilson, B. Alfarhani, A.F.T. Moore, C. Bisson, S.A. Wise, A.D. Campiglia, Determination of high-molecular weight polycyclic aromatic hydrocarbons in high performance liquid chromatography fractions of coal tar standard reference material 1597a via solid-phase nanoextraction and laser-excited time-resolved Shpol'skii spectroscopy, Talanta 148 (2016) 444–453, https://doi.org/10.1016/j.talanta.2015.11.018.
[5] M.S. García Falcón, S. González Amigo, M.A. Lage Yusty, J. Simal Lozano, Determination of benzo[a]pyrene in some Spanish commercial smoked products by HPLC-FL, Food Addit. Contam. 16 (1999) 9–14, https://doi.org/10.1080/026520399284271.
[6] L. Luo, S. Zhang, Y. Ma, Evaluation of impacts of soil fractions on phenanthrene sorption, Chemosphere 72 (2008) 891–896, https://doi.org/10.1016/j.chemosphere.2008.03.051.
[7] F.J. Stevenson, Humus Chemistry: Genesis, Composition, Reactions, 2nd ed. Wiley, New York, 1994.
[8] W. Zech, N. Senesi, G. Guggenberger, K. Kaiser, J. Lehmann, T.M. Miano, A. Miltner, G. Schroth, Factors controlling humification and mineralization of soil organic matter
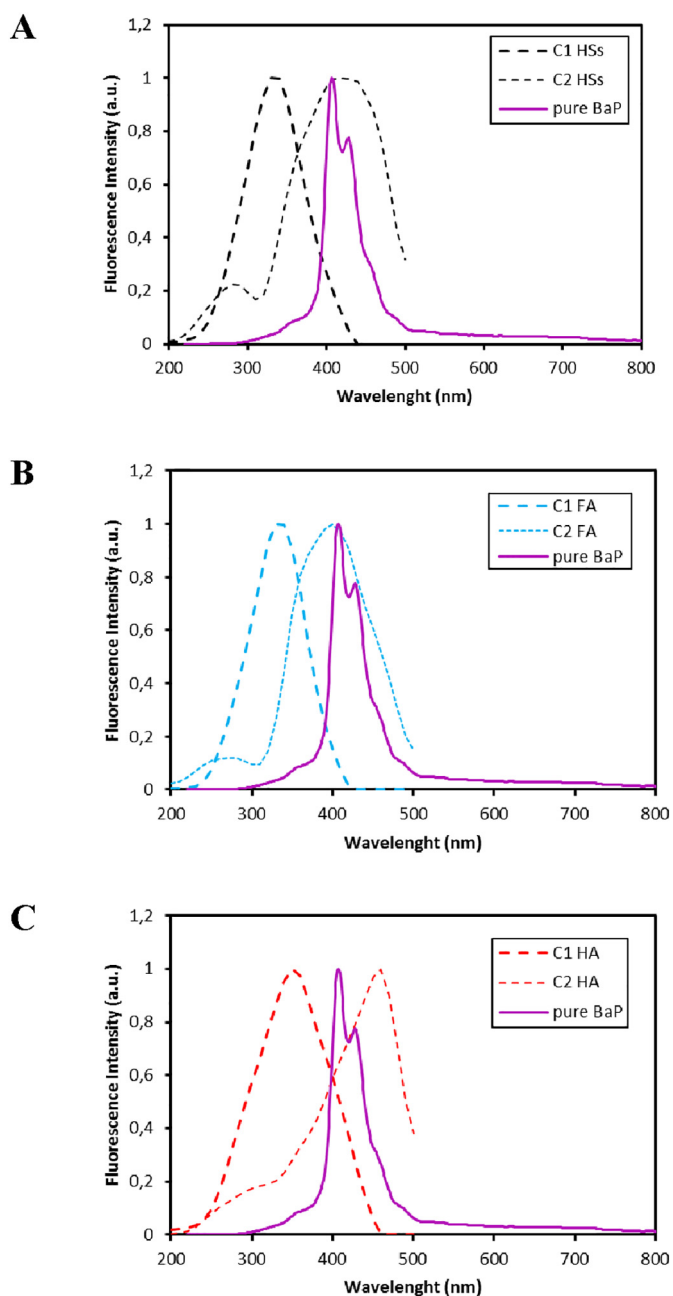
in the tropics, Geoderma 79 (1997) 117–161, https://doi.org/10.1016/S0016-7061 (97)00040-2.

[9] M. Klučáková, Characterization of pH-fractionated humic acids with respect to their dissociation behaviour, Environ. Sci. Pollut. Res. 23 (2016) 7722–7731, https://doi.org/10.1007/s11356-015-5932-2.

[10] M.M. Kononova, Soil Organic Matter: Its Nature, Its Role in Soil Formation and in Soil Fertility, Elsevier Science, Burlington, 2013http://public.eblib.com/choice/publicfullrecord.aspx?p=1817599, Accessed date: 3 May 2017.

[11] S. Bratskaya, A. Golikov, T. Lutsenko, O. Nesterova, V. Dudarchik, Charge characteristics of humic and fulvic acids: comparative analysis by colloid titration and potentiometric titration with continuous pK-distribution function model, Chemosphere 73 (2008) 557–563, https://doi.org/10.1016/j.chemosphere.2008.06.014.

[12] T. Michałowski, A.G. Asuero, New approaches in modeling carbonate alkalinity and total alkalinity, Crit. Rev. Anal. Chem. 42 (2012) 220–244, https://doi.org/10.1080/10408347.2012.660067.

[13] K.H. Tan, Humic Matter in Soil and the Environment: Principles and Controversies, second edition CRC Press, Taylor & Francis Group, Boca Raton, FL, 2014.

[14] V. Hernández-Montoya, L.H. Alvarez, M.A. Montes-Morán, F.J. Cervantes, Reduction of quinone and non-quinone redox functional groups in different humic acid samples by *Geobacter sulfurreducens*, Geoderma 183-184 (2012) 25–31, https://doi.org/10.1016/j.geoderma.2012.03.007.

[15] S. Huang, Y. Wang, L. Cao, K. Pi, M. Yu, E. Even, Multidimensional spectrofluorometry characterization of dissolved organic matter in arsenic-contaminated shallow groundwater, J. Environ. Sci. Health, Part A 47 (2012) 1446–1454, https://doi.org/10.1080/10934529.2012.672390.

[16] J.J. Pignatello, Soil organic matter as a nanoporous sorbent of organic pollutants, Adv. Colloid Interf. Sci. 76-77 (1998) 445–467, https://doi.org/10.1016/S0001-8686(98)00055-4.

[17] X. Qiu, S.I. Shah, E.W. Kendall, D.L. Sorensen, R.C. Sims, M.C. Engelke, Grass-enhanced bioremediation for clay soils contaminated with polynuclear aromatic hydrocarbons, in: T.A. Anderson, J.R. Coats (Eds.), Bioremediation Rhizosphere Technol. American Chemical Society, Washington, DC 1994, pp. 142–157, https://doi.org/10.1021/bk-1994-0563.ch013 (accessed March 20, 2017).

[18] J.F. McCarthy, L.E. Roberson, L.W. Burrus, Association of benzo(a)pyrene with dissolved organic matter: prediction of Kdom from structural and chemical properties of the organic matter, Chemosphere 19 (1989) 1911–1920, https://doi.org/10.1016/0045-6535(89)90014-3.

[19] P.F. Landrum, S.R. Nihart, B.J. Eadie, L.R. Herche, Reduction in bioavailability of organic contaminants to the amphipod *Pontoporeia hoyi* by dissolved organic matter of sediment interstitial waters, Environ. Toxicol. Chem. 6 (1987) 11–20, https://doi.org/10.1002/etc.5620060102.

[20] M. Haitzer, B.K. Burnison, S. Höss, W. Traunspurger, C.E.W. Steinberg, Effects of quantity, quality, and contact time of dissolved organic matter on bioconcentration of benzo[a]pyrene in the nematode *Caenorhabditis elegans*, Environ. Toxicol. Chem. 18 (1999) 459–465, https://doi.org/10.1002/etc.5620180314.

[21] C. Chen, J. Rubao, J.D. Schwab, D. Beletsky, L.G. Fahnenstiel, M. Jiang, T.H. Johengen, H. Vanderploeg, B. Eadie, J. Wells Budd, M.H. Bundy, W. Gardner, J. Cotner, P.J. Lavrentyev, A model study of the coupled biological and physical dynamics in Lake Michigan, Ecol. Model. 152 (2002) 145–168.

[22] T. Ohno, R. Bro, Dissolved organic matter characterization using multiway spectral decomposition of fluorescence landscapes, Soil Sci. Soc. Am. J. 70 (2006) 2028, https://doi.org/10.2136/sssaj2006.0005.

[23] P.G. Coble, S.A. Green, N.V. Blough, R.B. Gagosian, Characterization of dissolved organic matter in the Black Sea by fluorescence spectroscopy, Nature 348 (1990) 432–435, https://doi.org/10.1038/348432a0.

[24] P.G. Coble, Characterization of marine and terrestrial DOM in seawater using excitation-emission matrix spectroscopy, Mar. Chem. 51 (1996) 325–346, https://doi.org/10.1016/0304-4203(95)00062-3.

[25] A. Baker, Fluorescence excitation–emission matrix characterization of some sewage-impacted rivers, Environ. Sci. Technol. 35 (2001) 948–953, https://doi.org/10.1021/es000177t.

[26] J. Chen, E.J. LeBoeuf, S. Dai, B. Gu, Fluorescence spectroscopic studies of natural organic matter fractions, Chemosphere 50 (2003) 639–647, https://doi.org/10.1016/S0045-6535(02)00616-1.

[27] T. Marhaba, V. Doanh, R.L. Lippincott, Rapid identification of dissolved organic matter fractions in water by spectral fluorescent signatures, Water Res. 34 (2000) 3543–3550, https://doi.org/10.1016/S0043-1354(00)00090-7.

[28] T.F. Marhaba, Fluorescence technique for rapid identification of DOM fractions, J. Environ. Eng. 126 (2000) 145–152, https://doi.org/10.1061/(ASCE)0733-9372(2000)126:2(145).

[29] J. Chen, B. Gu, E.J. LeBoeuf, H. Pan, S. Dai, Spectroscopic characterization of the structural and functional properties of natural organic matter fractions, Chemosphere 48 (2002) 59–68, https://doi.org/10.1016/S0045-6535(02)00041-3.

[30] J. Gao, C. Liang, G. Shen, J. Lv, H. Wu, Spectral characteristics of dissolved organic matter in various agricultural soils throughout China, Chemosphere 176 (2017) 108–116, https://doi.org/10.1016/j.chemosphere.2017.02.104.

[31] M.M.D. Sierra, M. Giovanela, E. Parlanti, E.J. Soriano-Sierra, Fluorescence fingerprint of fulvic and humic acids from varied origins as viewed by single-scan and excitation/emission matrix techniques, Chemosphere 58 (2005) 715–733, https://doi.org/10.1016/j.chemosphere.2004.09.038.

[32] R.D. Holbrook, J.H. Yen, T.J. Grizzard, Characterizing natural organic material from the Occoquan Watershed (Northern Virginia, US) using fluorescence spectroscopy and PARAFAC, Sci. Total Environ. 361 (2006) 249–266, https://doi.org/10.1016/j.scitotenv.2005.11.020.

[33] R.G.M. Spencer, L. Bolton, A. Baker, Freeze/thaw and pH effects on freshwater dissolved organic matter fluorescence and absorbance properties from a number of UK locations, Water Res. 41 (2007) 2941–2950, https://doi.org/10.1016/j.watres.2007.04.012.

[34] J.L. Beltrán, R. Ferrer, J. Guiteras, Multivariate calibration of polycyclic aromatic hydrocarbon mixtures from excitation–emission fluorescence spectra, Anal. Chim. Acta 373 (1998) 311–319, https://doi.org/10.1016/S0003-2670(98)00420-6.

[35] N. Ferretto, M. Tedetti, C. Guigue, S. Mounier, R. Redon, M. Goutx, Identification and quantification of known polycyclic aromatic hydrocarbons and pesticides in complex mixtures using fluorescence excitation–emission matrices and parallel factor analysis, Chemosphere 107 (2014) 344–353, https://doi.org/10.1016/j.chemosphere.2013.12.087.

[36] R.D. JiJi, G.A. Cooper, K.S. Booksh, Excitation-emission matrix fluorescence based determination of carbamate pesticides and polycyclic aromatic hydrocarbons, Anal. Chim. Acta 397 (1999) 61–72, https://doi.org/10.1016/S0003-2670(99)00392-X.

[37] C.H. Santos, G. Nicolodelli, R.A. Romano, A.M. Tadini, P.R. Villas-Boas, C.R. Montes, S. Mounier, D.M.B.P. Milori, Structure of humic substances from some regions of the Amazon assessed coupling 3D fluorescence spectroscopy and CP/PARAFAC, J. Braz. Chem. Soc. (2015)https://doi.org/10.5935/0103-5053.20150076.

[38] A.M. Tadini, G. Nicolodelli, S. Mounier, C.R. Montes, D.M.B.P. Milori, The importance of humin in soil characterisation: a study on Amazonian soils using different fluorescence techniques, Sci. Total Environ. 537 (2015) 152–158, https://doi.org/10.1016/j.scitotenv.2015.07.125.

[39] R.A. Harshman, Foundations of the PARAFAC procedure: models and conditions for an "explanatory" multimodal factor analysis, UCLA Work. Pap. Phon. 16 1970, pp. 1–84.

[40] R. Bro, H.A.L. Kiers, A new efficient method for determining the number of components in PARAFAC models, J. Chemom. 17 (2003) 274–286, https://doi.org/10.1002/cem.801.

[41] C.A. Stedmon, R. Bro, Characterizing dissolved organic matter fluorescence with parallel factor analysis: a tutorial: fluorescence-PARAFAC analysis of DOM, Limnol. Oceanogr. Methods 6 (2008) 572–579, https://doi.org/10.4319/lom.2008.6.572.

[42] C.A. Stedmon, S. Markager, Resolving the variability in dissolved organic matter fluorescence in a temperate estuary and its catchment using PARAFAC analysis, Limnol. Oceanogr. 50 (2005) 656–697.

[43] C.M. Andersen, R. Bro, Practical aspects of PARAFAC modeling of fluorescence excitation-emission data, J. Chemom. 17 (2003) 200–215, https://doi.org/10.1002/cem.790.

[44] R. Bro, PARAFAC. Tutorial and applications, Chemom. Intell. Lab. Syst. 38 (1997) 149–171.

[45] A.M. Tadini, H. Hajjoul, G. Nicolodelli, S. Mounier, C.R. Montes, D.M.B.P. Milori, Characterization of organic matter in spodosol amazonian by fluorescence spectroscopy, World Acad. Sci. Eng. Technol. Int. Sci. Index 125, International J. Environ. Chem. Ecol. Geol. Geophys. Eng., vol. 11, 2017, pp. 322–325.

[46] W.-D. Guo, L.-Y. Yang, F.-L. Wang, W.-Z. Chen, X.-H. Wang, H.-S. Hong, Parallel factor analysis for excitation emission matrix fluorescence spectroscopy of dissolved organic matter from a reservoir-type river, Guang Pu Xue Yu Guang Pu Fen Xi Guang Pu 31 (2011) 427–430.

[47] M.L. Nahorniak, K.S. Booksh, Excitation-emission matrix fluorescence spectroscopy in conjunction with multiway analysis for PAH detection in complex matrices, Analyst 131 (2006) 1308, https://doi.org/10.1039/b609875d.

[48] R. Yang, N. Zhao, X. Xiao, S. Yu, J. Liu, W. Liu, Determination of polycyclic aromatic hydrocarbons by four-way parallel factor analysis in presence of humic acid, Spectrochim. Acta A Mol. Biomol. Spectrosc. 152 (2016) 384–390, https://doi.org/10.1016/j.saa.2015.07.094.

[49] P. Duchaufour, F. Jacquin, Nouvelles recherches sur l'extraction et le fractionnement des composes humiques, Bull. E.N.S.A. (1966) 3–24.

[50] C. Ratsimbazafy, Protocole de fractionnement et d'étude de la matière organique des sols hydromorphes de Madagascar, Cah. ORSTOMSérie, Pédologie 11 (1973) 227–236.

[51] S. Singh, E.J. D'Sa, E.M. Swenson, Chromophoric dissolved organic matter (CDOM) variability in Barataria Basin using excitation–emission matrix (EEM) fluorescence and parallel factor analysis (PARAFAC), Sci. Total Environ. 408 (2010) 3211–3222, https://doi.org/10.1016/j.scitotenv.2010.03.044.

[52] C.A. Stedmon, S. Markager, R. Bro, Tracing dissolved organic matter in aquatic environments using a new approach to fluorescence spectroscopy, Mar. Chem. 82 (2003) 239–254, https://doi.org/10.1016/S0304-4203(03)00072-0.

[53] R.M. Cory, D.M. McKnight, Fluorescence spectroscopy reveals ubiquitous presence of oxidized and reduced quinones in dissolved organic matter, Environ. Sci. Technol. 39 (2005) 8142–8149, https://doi.org/10.1021/es0506962.

[54] S. Nagao, T. Matsunaga, Y. Suzuki, T. Ueno, H. Amano, Characteristics of humic substances in the Kuji River waters as determined by high-performance size exclusion chromatography with fluorescence detection, Water Res. 37 (2003) 4159–4170, https://doi.org/10.1016/S0043-1354(03)00377-4.

[55] C.A. Stedmon, D.N. Thomas, M. Granskog, H. Kaartokallio, S. Papadimitriou, H. Kuosa, Characteristics of dissolved organic matter in Baltic Coastal Sea Ice: allochthonous or autochthonous origins? Environ. Sci. Technol. 41 (2007) 7273–7279, https://doi.org/10.1021/es071210f.

[56] B.J.H. Matthews, A.C. Jones, N.K. Theodorou, A.W. Tudhope, Excitation-emission-matrix fluorescence spectroscopy applied to humic acid bands in coral reefs, Mar. Chem. 55 (1996) 317–332, https://doi.org/10.1016/S0304-4203(96)00039-4.

[57] S. Nagao, Y. Suzuki, Y. Nakaguchi, M. Senoo, K. Hiraki, Direct measurement of the fluorescence characteristics of aquatic humic substances by a three-dimensional fluorescence spectrophotometer, Bunseki Kagaku 46 (1997) 335–342, https://doi.org/10.2116/bunsekikagaku.46.335.

[58] R.G. Zepp, W.M. Sheldon, M.A. Moran, Dissolved organic fluorophores in southeastern US coastal waters: correction method for eliminating Rayleigh and Raman

scattering peaks in excitation–emission matrices, Mar. Chem. 89 (2004) 15–36, https://doi.org/10.1016/j.marchem.2004.02.006.

[59] L.R. Tucker, A Method for the Synthesis of Factor Analysis Studies, Department of the Army, Washington, D.C., 1951

[60] M.J. Morra, M.O. Corapcioglu, R.M.A. von Wandruszka, D.B. Marshall, K. Topper, Fluorescence quenching and polarization studies of naphthalene and 1-naphthol

interaction with humic acid, Soil Sci. Soc. Am. J. 54 (1990) 1283, https://doi.org/10.2136/sssaj1990.03615995005400050014x.

[61] S. Chen, W.P. Inskeep, S.A. Williams, P.R. Callis, Fluorescence lifetime measurements of fluoranthene, 1-naphthol, and napropamide in the presence of dissolved humic acid, Environ. Sci. Technol. 28 (1994) 1582–1588, https://doi.org/10.1021/es00058a008.